JOURNAL OF SOLID STATE CHEMISTRY 63, 139–147 (1986)

Evolution of Three-Dimensional Character across the $La_{n+1}Ni_nO_{3n+1}$ Homologous Series with Increase in n[1]

R. A. MOHAN RAM, L. GANAPATHI, P. GANGULY, AND C. N. R. RAO[2]

Solid State and Structural Chemistry Unit, Indian Institute of Science, Bangalore 560 012, India

Received July 10, 1985; in revised form October 25, 1985

Electrical and magnetic properties of $La_3Ni_2O_7$ and $La_4Ni_3O_{10}$ have been investigated in comparison with those of La_2NiO_4, $LaNiO_3$, and $LaSrNiO_4$. The results suggest an increasing 3-dimensional character across the homologous series $La_{n+1}Ni_nO_{3n+1}$ with increase in n. Accordingly, the electrical resistivity decreases in the order $La_3Ni_2O_7$, $La_4Ni_3O_{10}$, and $LaNiO_3$ and this trend is suggested to be related to the percolation threshold. Magnetic properties of these oxides also show some interesting trends across the series.

I. Introduction

$LaNiO_3$ possessing the perovskite structure is Pauli pramagnetic and metallic. The two-dimensional La_2NiO_4, on the other hand, possesses the K_2NiF_4 structure with layers of $LaNiO_3$ being present in between rock-salt type LaO layers; this oxide exhibits a semiconductor–metal transition around 500 K in the *ab* plane (*1*). Stoichiometric La_2NiO_4 also shows an anomaly in the magnetic susceptibility around 200 K (*2*). $LaNiO_3$ and La_2NiO_4 can form a homologous series of oxides of the general formula $La_{n+1}Ni_nO_{3n+1}$ similar to the Ruddlesdon–Popper series of oxides formed by $SrTiO_3$ and Sr_2TiO_4 (*3*, *4*). The first two members of such a homologous series are $La_3Ni_2O_7$ with $n = 2$ and $La_4Ni_3O_{10}$ with $n = 3$ (*4–6*). We considered it important to investigate how the two-dimensional electronic and magnetic properties of La_2NiO_4 transform to three-dimensional behavior with an increase in the number of $LaNiO_3$ layers (the value of n) across the homologous series. We have investigated the problem by examining the electric, magnetic, and other properties of the $n = 2$ and $n = 3$ members in comparison with those of La_2NiO_4.

2. Experimental

La_2NiO_4 was prepared by decomposing stoichiometric amounts of the lanthanum and nickel nitrates and heating at 1470 K for 24 hr. The compound was pelletized and heated at 1470 K for 24 hr with intermittent grinding. Stoichiometric La_2NiO_4 was prepared by heating the above sample at 1470 K in CO_2 atmosphere for 12 hr. $La_3Ni_2O_7$ was prepared by decomposing stoichiometric amounts of lanthanum and nickel ni-

[1] Contribution No. 304 from the Solid State and Structural Chemistry Unit.

[2] To whom all correspondence should be addressed.

0022-4596/86 $3.00

trates and heating at 1420 K for 10 hr with frequent grinding. $La_4Ni_3O_{10}$ was prepared by the hypochlorite method as follows. Stoichiometric amounts of lanthanum and nickel nitrates were added to a concentrated solution of sodium hydroxide through which chlorine gas was bubbled. The precipitate thus obtained was washed with hot water and filtered several times till the filtrate showed a pH of 7. The residue was then heated at 1350 K for 5 hr. Sodium ions if present in the sample are beyond the levels of detection.

The formation of single phases of all the compounds was ascertained by X-ray diffraction studies using a Phillips PW-1050 X-ray diffractometer with Cu$K\alpha$ radiation. Stoichiometry of the compounds was established by iodometric titrations and chemical analysis. Titrable oxygen could be determined to an accuracy of 0.1% by suitably changing the amount of substance taken and the strength of the thiosulphate solution. Estimates of La/Ni ratio on representative samples correspond to the expected values. The stoichiometric sample of La_2NiO_4 has a monoclinic unit cell as reported earlier (*1*). $La_3Ni_2O_7$ had the unit cell parameters a = 5.412 Å, b = 5.456 Å, and c = 20.94 Å, $La_4Ni_3O_{10}$ gave the unit cell parameters a = 5.424 Å, b = 5.478 Å, and c = 28.07 Å, the increase in the c parameter of this oxide compared to $La_3Ni_2O_7$ being as expected. The unit cell parameters are comparable to those reported by Drennan (*4*).

High-resolution electron microscopic (HREM) studies were made using a JEOL JEM-200 CX transmission electron microscope operating at 200 keV and equipped with an ultra-high-resolution objective pole piece (C_s = 1.2 mm) in the top-entry configuration. Crystallites of different materials were dispersed on a holey carbon grid. Thin crystals projecting through the holes were brought to the required orientation with the help of the goniometer. Through-focus images with defocus values up to 120 nm were recorded at a primary magnification in the range 3×10^5–5×10^5.

Magnetic susceptibility measurements were carried out by employing the Faraday technique using a Cahn-RG electrobalance and using $Hg[Co(SCN)_4]$ as the calibrant. Electrical resistivity measurements were made by the four-probe method using an indigenous apparatus. Pellets sintered at 1100 K in oxygen atmosphere were used.

3. Results

Structural images. La_2NiO_4 with a tetragonal structure should give a simple electron diffraction pattern and a HREM image. Since there is always a certain excess of oxygen (sometimes even up to 9%) in La_2NiO_4 samples, presence of the higher (n = 2 or 3) members of the $La_{n+1}Ni_nO_{3n+1}$ series has been suspected (*4*, *7*). However, a study of number of La_2NiO_4 crystals by high-resolution electron microscopy (HREM) did not show the presence of any of the higher members in our samples (Fig. 1). HREM studies of $La_3Ni_2O_7$ (n = 2) and $La_4Ni_3O_{10}$ (n = 3) showed the presence of ordered structures with the expected recurrence of perovskite layers over large distances. In Fig. 2, we have shown lattice images of $La_3Ni_2O_7$ and $La_4Ni_3O_{10}$ to demonstrate recurrent ordered intergrowth. In this figure we have also shown the corresponding electron diffraction patterns and the structural projections. In some crystals of these oxides, we have encountered disordered intergrowth of different members. For example, in Fig. 3 we have shown the lattice image of $La_3Ni_2O_7$ which shows occasional presence of the n = 3 and n = 5 members. The average value of n corresponds, however, to the value expected for the starting composition (n = 2) and the diffraction patterns (see Fig. 3) show no evidence for the presence of the $n > 2$ members. Such random intergrowth of $n \neq 3$

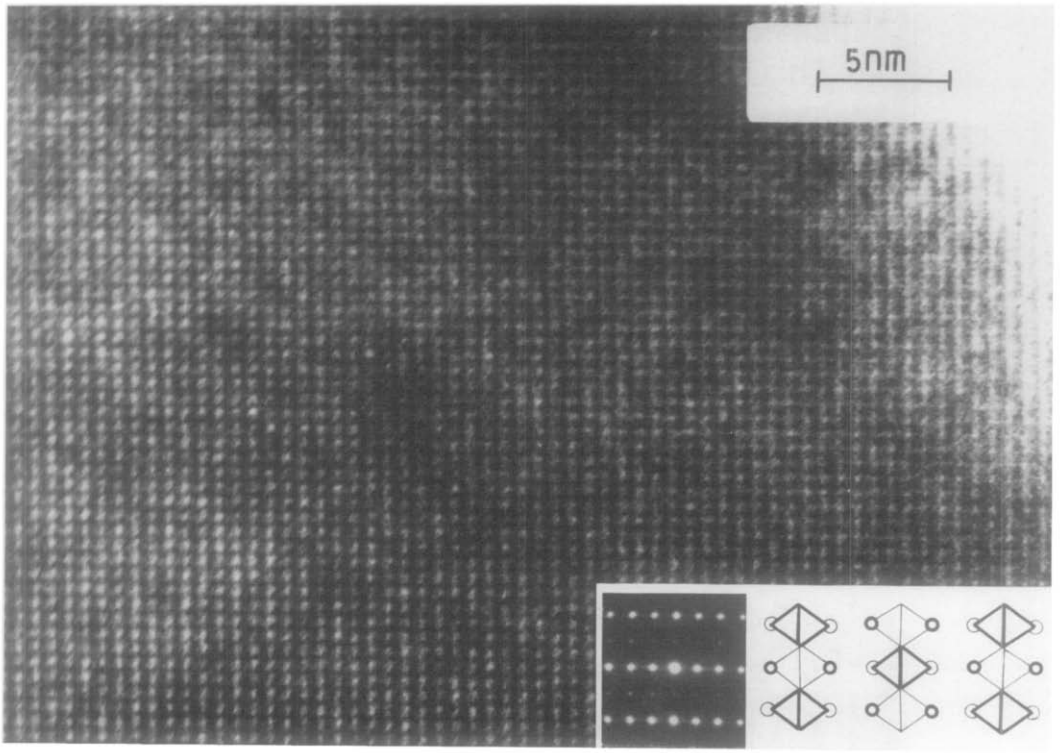

FIG. 1. HREM image of La_2NiO_4 along [100]. The inset shows structural projection and the electron diffraction pattern.

members were also observed for the $n = 3$ member $La_4Ni_3O_{10}$ (Fig. 4). The present study suggests that for all practical purposes, $La_3Ni_2O_7$ and $La_4Ni_3O_{10}$ samples can be considered to be monophasic on average, possessing the expected intergrowth structures in spite of the presence of occasional disorder. We would therefore expect properties of these oxides to reflect the features expected of the $n = 2$ and $n = 3$ members of the homologous series.

A comment on intergrowth structures (*8*) would be appropriate. The fact that different members of a homologous series of oxides can coexist shows that although they differ compositionally, the intergrowth is facilitated by the similarity of the interface (*ab* plane in the present case) which has similar dimensions and structure in the members. Whenever such proper registry is favored across the interface, intergrowths occur readily. Accordingly, an amazing series of recurrent intergrowth structures is formed by the Aurivillius family of oxides (*9*); in these intergrowths, the HREM studies have provided vital information on the presence and the nature of elastic strain at the solid–solid interface (*10*).

Electrical properties. Plots of the logarithm of electrical resistivity against temperature for $LaSrNiO_4$, $La_3Ni_2O_7$. $La_4Ni_3O_{10}$ and $LaNiO_3$ are shown in Fig. 5. In the series $La_3Ni_2O_7$, $La_4Ni_3O_{10}$, and $LaNiO_3$, there is a progressive decrease in the resistivity with an increase in the percentage of Ni^{3+}. It may be argued that the decrease in the resistivity is due to the increasing Ni^{3+} content; however, $LaSrNiO_4$

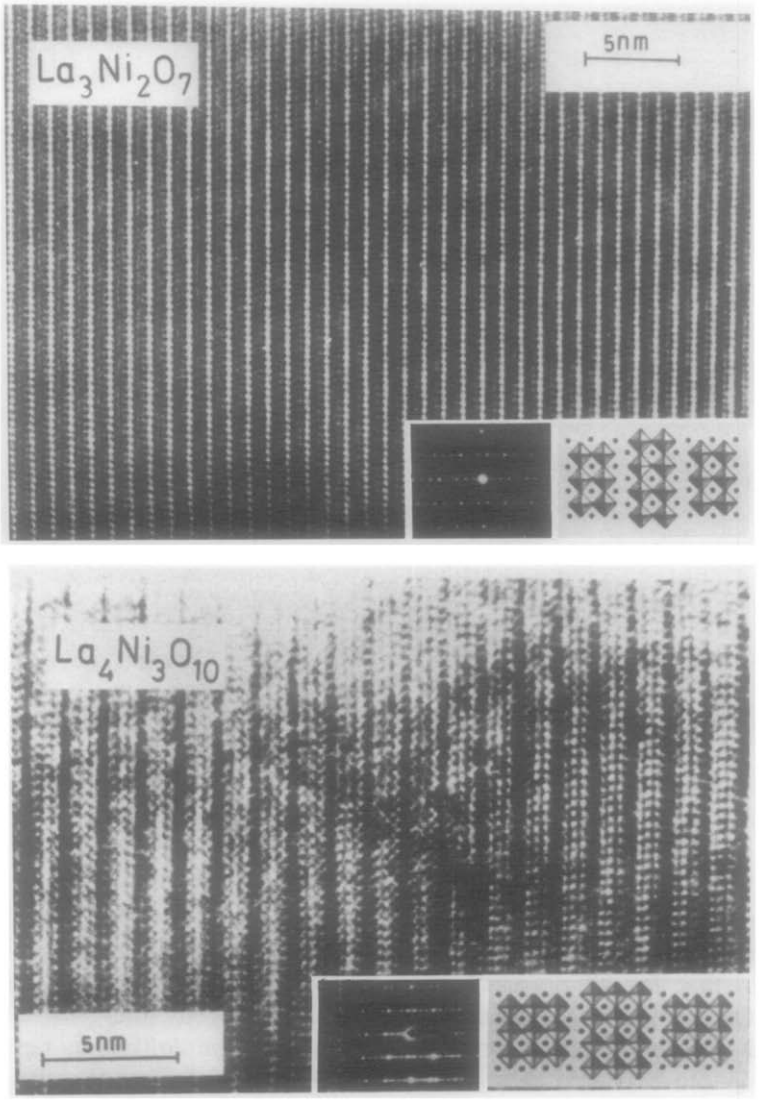

FIG. 2. HREM images of $La_3Ni_2O_7$ and $La_4Ni_3O_{10}$ along $[\bar{1}10]$ showing recurrent intergrowth structures. The inset show structural projections and the electron diffraction patterns.

where the nickel ions are in the 3+ state exhibits high resistivity compared to $La_3Ni_2O_7$ or $La_4Ni_3O_{10}$. It would thus seem that the increase in the number of perovskite layers has a role to play in decreasing the resistivity of $n = 2$ and $n = 3$ members of the $La_{n+1}Ni_nO_{3n+1}$ system. It is known that the lowering of the dimensionality increases the resistivity of the system. Accordingly, the resistivity of $LaSrNiO_4$ is two orders of magnitude higher than $LaNiO_3$. $La_{0.5}Sr_{1.5}CoO_4$ (also written as $SrO \cdot La_{0.5}Sr_{0.5}CoO_3$) which has the K_2NiF_4 structure and is the two-dimensional analog of the itinerant electron ferromagnet $La_{0.5}Sr_{0.5}CoO_3$ exhibits very high resistivity. This supports the view that the increase in dimensionality increases the conductiv-

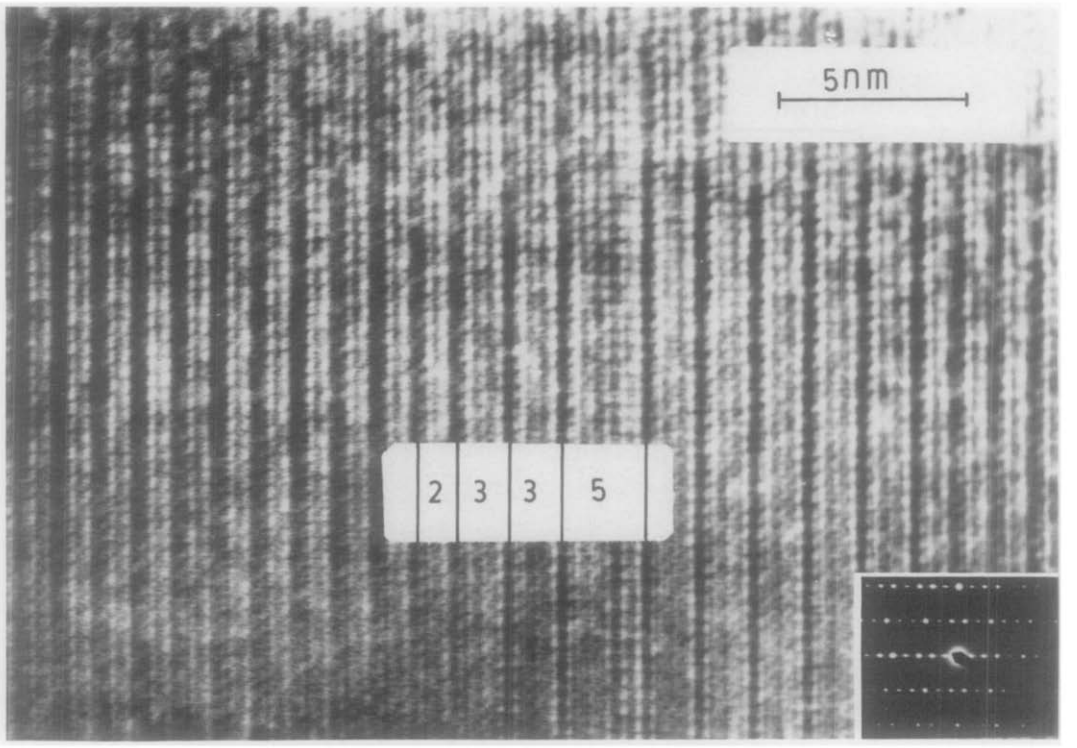

FIG. 3. HREM image of $La_3Ni_2O_7$ along [$\bar{1}$10] showing disordered intergrowth. Electron diffraction pattern is also shown.

ity. The temperature dependence of the n = 2 and n = 3 samples in the present study indicates metallic behavior although the value of the resistivity is greater than the limiting value of resistivity ($\sim 2 \times 10^{-3}$ ohm cm^{-1}), which separates insulating (negative TCR) and metallic (positive TCR) phases of oxides of the type $LaNi_{1-x}B_xO_3$ where B = Fe, Cr, or Mn (*11, 12*). The discrepancy may be attributed to the anisotropy in conductivity parallel and perpendicular to the perovskite layers as observed in La_2NiO_4 (*1*).

Magnetic properties. The temperature-variation of the inverse magnetic susceptibility (per gram atom of nickel), χ_{Ni}^{-1}, of nearly stoichiometric and slightly oxidized samples of La_2NiO_4 ($La_2NiO_{4.002}$ and $La_2NiO_{4.11}$, respectively) as well as $LaNiO_3$, $La_3Ni_2O_7$, $La_4Ni_3O_{10}$, and $LaSrNiO_4$ are shown in Figs. 6 and 7. The susceptibility of $La_2NiO_{4.002}$ is much lower than that of $La_2NiO_{4.11}$ and shows an anomaly around 200 K; a more pronounced anomaly is found in annealed, stoichiometric single crystals of La_2NiO_4 (*2*) as shown in the inset of Fig. 6. The lower magnitude of the susceptibility of stoichiometric La_2NiO_4 can be attributed to the increase in the strength of antiferromagnetic interactions. The χ_{Ni}^{-1} vs T plot of $La_2NiO_{4.002}$ above 200 K does not obey the Curie–Weiss law and is fairly independent of temperature, suggesting that there is considerable antiferromagnetic correlation present above 200 K.

4. Discussion

The interesting aspect of the susceptibility data of the $La_{n+1}Ni_nO_{3n+1}$ samples is that the below-room-temperature susceptibility

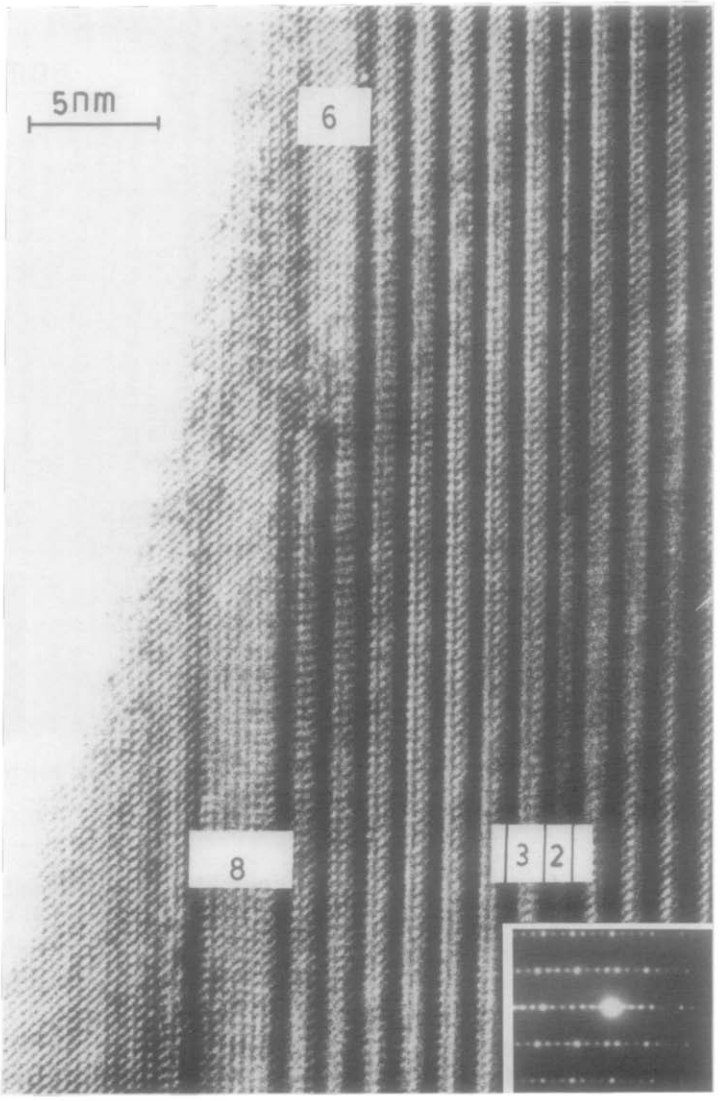

FIG. 4. HREM image of $La_4Ni_3O_{10}$ along [$\bar{1}$10] showing disordered intergrowth. Electron diffraction pattern is also shown.

per gram atom of Ni is nearly the same despite the large changes in the resistivity and in the formal oxidation state of nickel (Fig. 7). This suggests that there is considerable antiferromagnetic ordering probably of short range. Since long-range antiferromagnetic ordering is usually seen when the Coulomb correlation energy is high (when electrons are localized), the absence of features associated with long-range in the $n = 2$ and $n = 3$ systems implies a small correlation energy consistent with the observation that these oxides are nearly itinerant electron systems.

Some of the important features that are of interest in the present study are the following: (i) magnetic susceptibilities of the $La_{n+1}Ni_nO_{3n+1}$ samples in the 100–300 K

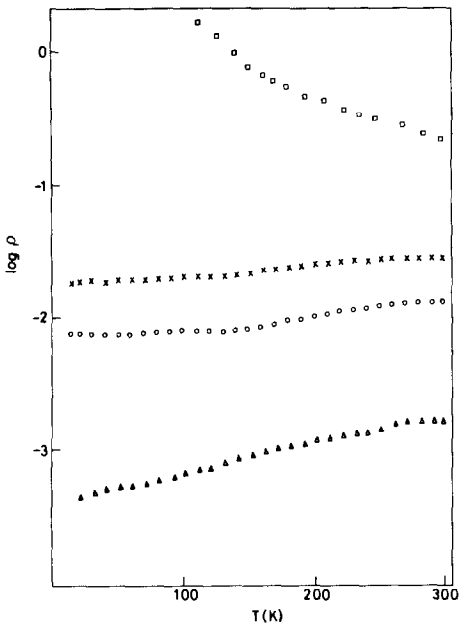

FIG. 5. Plots of log ρ vs T (K) for $LaSrNiO_4$ (squares), $La_3Ni_2O_7$ (crosses), $La_4Ni_3O_{10}$ (circles), and $LaNiO_3$ (triangles).

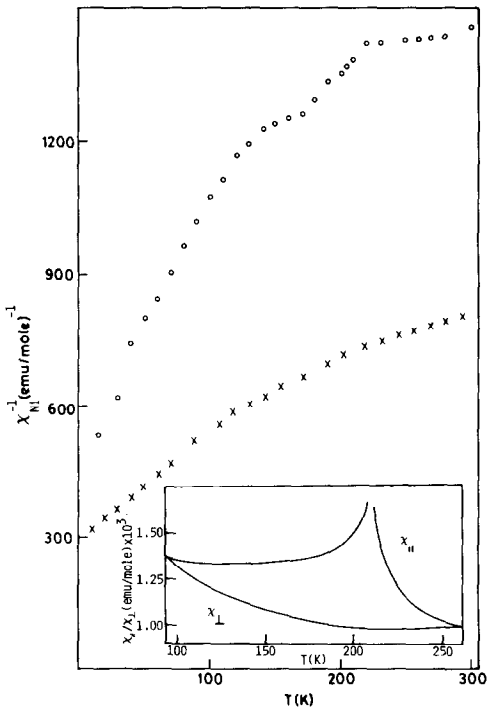

FIG. 6. Plots of χ_{Ni}^{-1} vs T (K) for $La_2NiO_{4.002}$ (circles) and $La_2NiO_{4.11}$ (crosses). Inset shows plot for the single crystal of stoichiometric La_2NiO_4 (2).

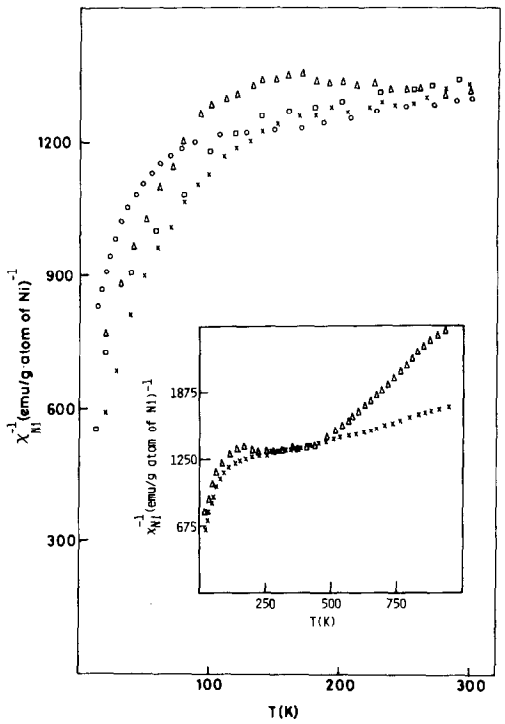

FIG. 7. Plots of χ_{Ni}^{-1} vs T (K) for $LaSrNiO_4$ (squares), $La_3Ni_2O_7$ (crosses), $La_4Ni_3O_{10}$ (circles), and $LaNiO_3$ (triangles).

range seem to be simply the sum of the susceptibilities of $(n-1)$ $LaNiO_3$ and La_2NiO_4 as if the Ni^{3+} and Ni^{2+} are seggregated in different layers. This would suggest that the $n = 2$ and $n = 3$ members can be described as $LaNiO_3 \cdot La_2NiO_4$ and $2LaNiO_3 \cdot La_2NiO_4$, respectively. (ii) The $n = 2$ sample shows evidence for short-range ordering at low temperatures when the susceptibility over the entire temperature range is taken into account (see inset of Fig. 7). From the slope of the χ_{Ni}^{-1} vs T plot, the calculated value of the Curie constant works out to be only 0.47 emu K/g atom of Ni. This value is too small to be accounted for by the presence of localized moments on all the Ni ions. Instead, the observed value may roughly be accounted for if it is assumed that only Ni^{2+} ions contribute to the localized moment while the electrons of Ni^{3+} do not contribute to the temperature-

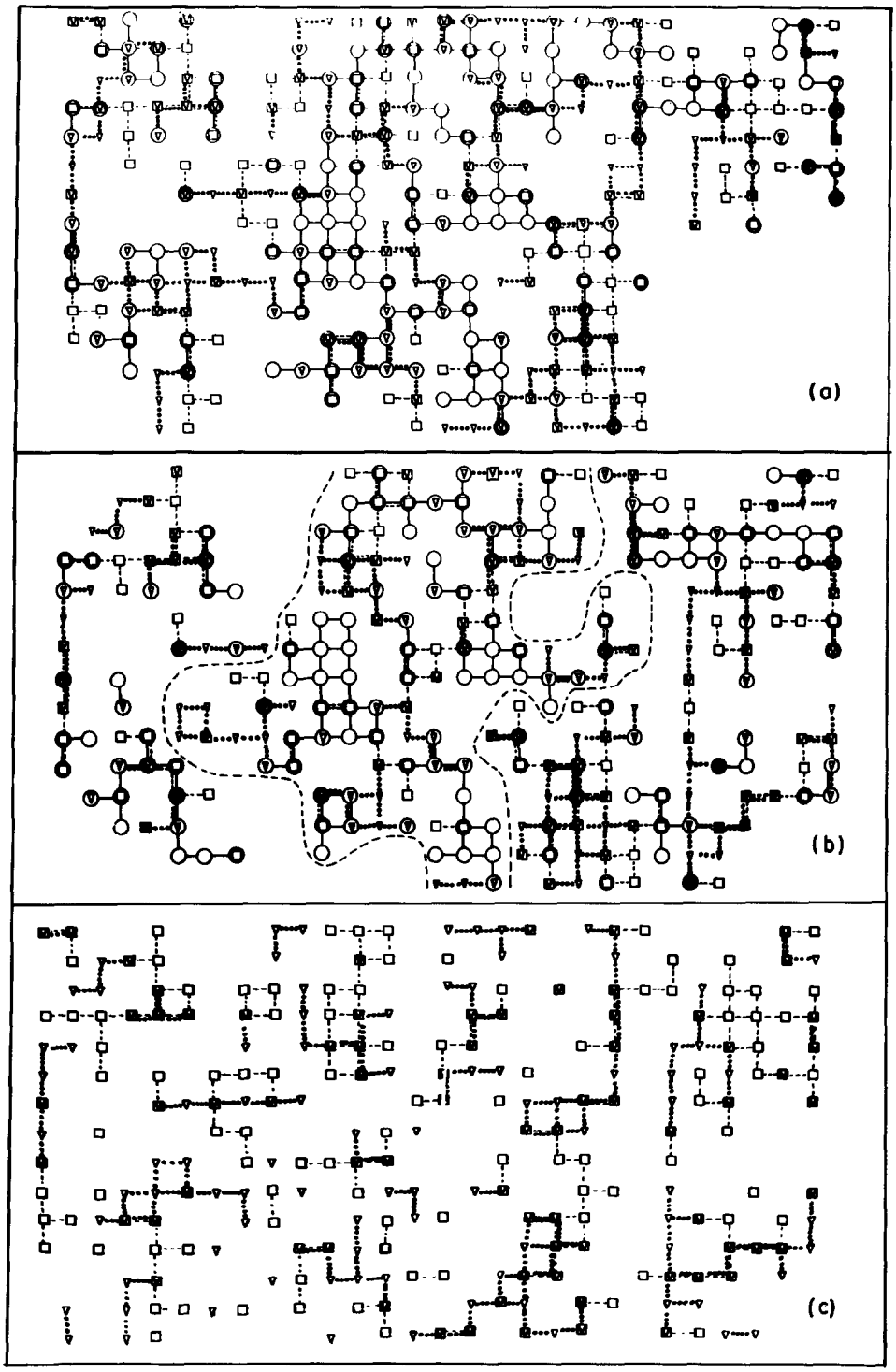

FIG. 8. Nearest-neighbor connected sites of Ni^{3+} for different layers indicated by squares, triangles, and circles. For three layers the squares correspond to the central plane. (a) Three layers with 55% Ni^{3+}; (b) three layers with 50% Ni^{3+}; (c) two layers with 55% Ni^{3+}.

dependent part of the susceptibility. On the other hand, the high-temperature Curie constant of the $n = 3$ sample (~0.6 emu K/g atom of Ni) is much higher and corresponds to the value anticipated if all the nickel ions were to contribute to the temperature-dependent part of the susceptibility. This difference in the behavior of the $n = 2$ and $n = 3$ samples is partly resolved if the temperature-independent susceptibility found in $LaNiO_3$ makes the predominent contribution in the case of the $n = 3$ sample. The only systematic change found in the low-temperature behavior was in the slopes of the χ_M^{-1} vs T plots. From the Curie–Weiss plots below 80 K the value of the Curie constants for the $n = 2$, 3, and ∞ compositions are, respectively, 0.14, 0.10, and 0.008 emu K/g atom of Ni) while the paramagnetic Curie temperatures are, respectively 100, 40, and 5 K. The increase in susceptibility at low temperatures may also be attributed to the formation of spin polarons in the model proposed by Mott (see Fig. 7 of Ref. (*13*)). We note that $LaSrNiO_4$ which has a higher resistivity than $LaNiO_3$ also shows a more enhanced susceptibility at low temperatures.

The difference in the magnetic and electrical properties of the $n = 2$ and $n = 3$ samples may also be examined in terms of percolation effects. For a two-dimensional square planar array, the site percolation threshold is 60% (*14*). In the $LaSrAl_{1-x}Ni_xO_4$ system possessing the K_2NiF_4 structure, evidence has been presented for the delocalization of the e_g electrons of the Ni^{3+} ion when $x > 0.6$ (*15*). The critical site percolation threshold for $n = 2$ and $n = 3$ layers of a square planar array has not been studied in the literature. A visual inspection of random arrays of various concentrations for the $n = 2$ and $n = 3$ layers showed that the critical site percolation threshold is between 55 and 60% for $n = 2$ and between 50 and 55% for $n = 3$ (Fig. 8). Thus, for the $n = 2$ member, the concentration of Ni^{3+} (50%) is below the critical percolation threshold estimated by us while for the $n = 3$ member, the concentration of the Ni^{3+} (66%) ion is above the critical percolation threshold.

Acknowledgments

The authors thank the University Grants Commission and the Department of Science and Technology, Government of India, for support of this research.

References

1. C. N. R. Rao, D. Buttrey, N. Otsuka, P. Ganguly, H. R. Harrison, C. J. Sandberg, and J. M. Honig, *J. Solid State Chem.* **51,** 266 (1984).
2. D. Buttrey, J. M. Honig, and C. N. R. Rao, *J. Solid State Chem.* to be published.
3. R. J. D. Tilley, *J. Solid State Chem.* **21,** 293 (1977).
4. J. Drennan, C. P. Tavares, and B. C. H. Steele, *Mater. Res. Bull.* **17,** 621 (1982).
5. M. Seppanen, *Scand. J. Metall.* **8,** 191 (1979).
6. C. Brish, M. Vallino, and F. Abbattista, *J. Less-Common Met.* **79,** 215 (1981).
7. P. Odier, Y. Nigara, J. Contures, and M. Sayer, *J. Solid State Chem.* **56,** 32 (1985).
8. C. N. R. Rao and J. M. Thomas, *Acc. Chem. Res.* **18,** 113 (1985).
9. J. Gopalakrishnan, A. Ramanan, C. N. R. Rao, and D. A. Jefferson, *J. Solid State Chem.* **55,** 101 (1984).
10. D. A. Jefferson, M. K. Uppal, C. N. R. Rao, and D. J. Smith, *Mater. Res. Bull.* **19,** 1403 (1984).
11. P. Ganguly, N. Y. Vasanthacharya, C. N. R. Rao, and P. P. Edwards, *J. Solid State Chem.* **54,** 400 (1984).
12. C. N. R. Rao and P. Ganguly, *in* "Metal-Insulator Transitions" (D. Adler and H. Fritzsche, Eds.), Plenum, New York, 1985.
13. N. F. Mott, *Adv. Phys.* **21,** 785 (1972).
14. B. K. Shante and S. Kirkpatrick, *Adv. Phys.* **20,** 325 (1971).
15. R. A. Mohan Ram, K. K. Singh, W. H. Madhusudan, P. Ganguly, and C. N. R. Rao, *Mater. Res. Bull.* **18,** 703 (1983).